Theoretical investigation of sensitivity enhancement by using gold nanoparticles in a sensing layer and 2D-nanomaterials in SPR biosensor

SAEED GHORBANI*, MOJTABA SADEGHI*, ZAHRA ADELPOUR
Department of Electrical Engineering, Shiraz Branch, Islamic Azad University, Shiraz, Iran

The all-optical biosensor based on Surface Plasmon Resonance (SPR) with improved sensitivity is introduced which exploits theoretical analysis and simulation of biomaterial detection in liquids. A five-layer Kretschmann configuration is considered with emphasis on nanocomposite structure of sensing layer along with extra two-dimensional (2D) layer. Sensing layer consists of gold nanoparticles with biomaterial sample shell. Moreover, different types of 2D material (graphene, Black Phosphorous (BP) and tungsten disulfide (WS2)) with variable thickness are considered beneath the sensing layer. Comprehensive simulations based on Maxwell-Garnett theory are done to fully investigate the nanocomposite physical characteristics effect, thickness and the type of 2D material layer on biosensor performance. It is concluded that in the case of $5nm$ core radius, $5nm$ shell thickness and 0.1 filling factor, the improved sensitivity value of 260.385 $\left(^{\circ}/_{RIU}\right)$ is achievable if a $24nm$ layer of WS2 2D material is added beneath the sensing layer. The proposed biosensor has a high sensitivity being capable of real-time monitoring the samples. By considering the special characteristics of the proposed biosensor, this biosensor can be considered as a good candidate for biomaterial sample detection in liquids.

(Received May 12, 2021; accepted April 8, 2022)

Keywords: Optical biosensor, Surface plasmon resonance, Sensitivity, Core-shell nanostructure, Nonocomposite, Maxwell-Garnett theory

1. Introduction

Many studies have been done during the last years in order to improve and develop the performance of optical biosensors in a variety of practical fields such as medicine, pharmacy, food industry, etc [1-4]. Because of high accuracy and sensitivity, fast and real-time response, the optical sensors are among the ever-rising technologies for detection and sensing [5-7]. The physical phenomenon of Surface Plasmon Resonance (SPR) [8-9] is widely used in the design of optical biosensor with high sensitivity and performance to detect biomolecules and biomaterial sample in liquid [10-12].The performance of these biosensors are based on measuring the refractive index (RI) changes of the biomaterial sample in liquid [10]. Moreover, the plasmonic nanoparticles are used as the active material in the sensing layer of the biosensor to increase the detection and sensitivity of biosensors [13-16]. In multilayer SPR biosensors, Otto [17-18] and Kretschmann [19] configurations, operating in two modes of angular and wavelength investigation, have attracted much attention. These two configurations are employed in order to excite the Surface Plasmon Polariton (SPP) waves at the interface of metal and dielectric as the sensing layer. Nanomaterials are widely used to increase the sensitivity and improve the performance of biosensor.

Besides, due to the unique electrical, optical, and mechanical characteristics of 2D materials such as graphene [20], Black Phosphorous (BP) [21-22] and transition metal dichalcogenides (TMDCs),i.e.,$MoS_2, MoSe_2, WSe_2$ *and* WS_2 [23], they are used as a thin layer on the metal layer in some studies to enhance the sensitivity, detection accuracy and quality factor of SPR biosensor[24-26]. These materials have a high surface area to volume ratio so, the performance of the SPR biosensors are improved.

Rahman et al. have investigated two configurations of $Ag/PtSe_2/WS_2$ and $Au/PtSe_2/WS_2$ based on SPR biosensors with sensitivity of 194 $\left(^{\circ}/_{RIU}\right)$ and 187 $\left(^{\circ}/_{RIU}\right)$ [27]. Also, Lin et al. have proposed SPR biosensor with $SF11/Au/MoS_2/WS_2/WSe_2$, $SF11/Cu/WSe_2$ and $SF11/Cu/graphene$ configurations. The sensitivity of these nanostructures are $142\left(^{\circ}/_{RIU}\right), 92\left(^{\circ}/_{RIU}\right)$ *and* 194 $\left(^{\circ}/_{RIU}\right)$, respectively [28]. These reports show that 2D-nanomaterials increase the sensitivity and improve the performance of biosensors.

In this study, a SPR biosensor with multi-layer Kretschmann configuration having high performance and sensitivity is proposed for biomaterial sample detection in liquids. The configuration of the proposed biosensor and theoretical methods are described in section 2. In section 3, the simulation results are presented along with the discussions. And the paper is finished by the conclusion part in section 4.

2. Models and method

In Fig. 1, the proposed SPR biosensor with a five-layer Kretschmann configuration is shown. The operating wavelength is set to $633nm$. In Kreschmann configuration SPR biosensor, the resonant angle is very important and it is necessary to select each layer properly. The first layer of the structure is SF10 with refractive index of 1.7283 at operating wavelength as the exciting prism [29]. A layer of silver with thickness of $20nm$ is deposited on the prism to excite the SPP waves. The wavelength-dependent refractive index of silver layer using the Drude-Lorentz model in the form of $n_{Ag} = \sqrt{1 - \frac{\lambda^2 \lambda_c}{\lambda_p^2(\lambda_c + i\lambda)}}$ is used in our simulation. Where, $\lambda_p$is the plasma wavelength, and $\lambda_c$is the collision wavelength, which is $1.4541 \times 10^{-7}m$and $1.7614 \times 10^{-5}m$for silver, respectively [30]. So, the refractive index of silver layer is $n_{Ag} = 0.218 + 3.512i$ at 633nm.

The third layer consists of a thin layer of 2D material which is coated on the silver layer. This thin layer prevents the metal layer from oxidation. The refractive index and thickness of 2D materials used in this paper are presented in Table 1, where L, M and N are the number of each layer. According to real part of refractive index, these materials have great ability to absorb the incoming light energy.

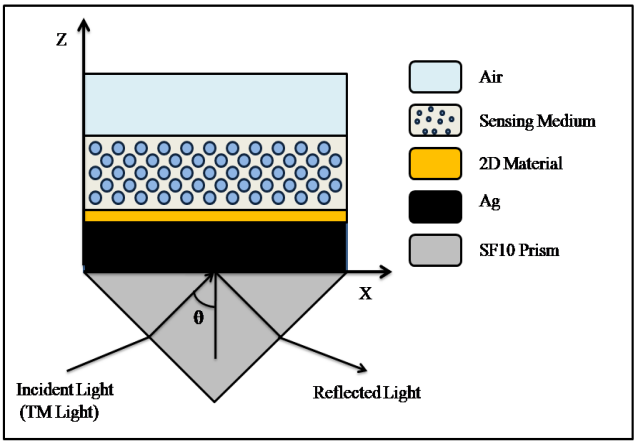

Fig. 1. The proposed SPR biosensor with Kretschmann configuration (color online)

Table 1. Physical parameters of three different types of 2D material at $\lambda = 633nm$

Type of 2D Materials	Graphene[31]	Black phosphorous(BP)[22]	Tungsten disulfide(WS2)[32]
Thickness of layer(nm)	L×0.34	M×0.53	N×0.8
Refractive Index	3+1.1491i	3.5+0.01i	4.9+0.3124i

The thickness of sensing medium is set to $100nm$ as the forth layer in the proposed structure and it is modelled as a nanocomposite layer consisting of nanoparticles with Core-Shell (Au-biomaterial sample) structure, which are randomly distributed in a host medium [33-34].

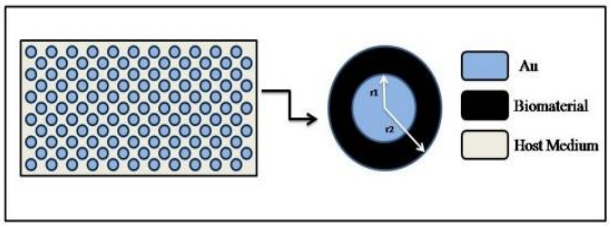

Fig. 2. The nanocomposite layer containing nanoparticles with core-shell structure (color online)

Fig. 2 shows the structure of the nanocomposite layer as the sensing medium. It is shown that nanoparticles consist of a gold core with radius r_1 and biomaterial sample with thickness $a = r_2 - r_1$ which are distributed evenly in the host medium.

The refractive index of gold nanoparticles is expressed as $n_{Au} = \sqrt{1 - \frac{\lambda^2 \lambda_c}{\lambda_p^2(\lambda_c + i\lambda)}}$, in which λ_p and λ_c for gold are 1.6826×10^{-7}m and $8.9342 \times 10^{-6}m$, respectively [30]. So, the refractive index of gold nanoparticle is $n_{Au} = 0.172 + 3.422i$ at 633nm.The refractive index of biomaterial sample and host medium is set to $n_{Bio} = 1.35$ and $n_{host} = 1.33$ (refractive index of pure water), respectively. It is assumed that the size of nanoparticles is smaller than the incident light wavelength, and so the Rayleigh's theory of scattering can be ignored, and consequently, the effective dielectric constant of nanoparticles, shown in Fig. 2, can be expressed as [35-36]

$$\varepsilon_e = \varepsilon_2 \frac{r_2^3(\varepsilon_1 + 2\varepsilon_2) + 2r_1^3(\varepsilon_1 - \varepsilon_2)}{r_2^3(\varepsilon_1 + 2\varepsilon_2) - r_1^3(\varepsilon_1 - \varepsilon_2)} \quad (1)$$

where, ε_1 and ε_2 are the dielectric constant of gold and biomaterial sample. $r_1$and r_2 are the core radius and core shell, respectively.

According to Equation 1, the effective dielectric constant of nanoparticles with core-shell structure is dependent on the radius and dielectric constant of core (gold) and shell (biomaterial sample).

To include the effect of hosting medium in simulation, the Maxwell-Garnett theory [37-38] is used to model and calculate the effective dielectric constant of the sensing layer as [39]

$$\varepsilon = \varepsilon_3 + 3f\varepsilon_3 \frac{\varepsilon_2\varepsilon_a - \varepsilon_3\varepsilon_b}{\varepsilon_2\varepsilon_a + 2\varepsilon_3\varepsilon_b} \quad (2)$$

Where

$$\frac{\varepsilon_e + 2\varepsilon_3}{\varepsilon_e - \varepsilon_3} = f\frac{\varepsilon + 2\varepsilon_3}{\varepsilon - \varepsilon_3} \quad (3)$$

$$\varepsilon_a = \varepsilon_1(3 - 2P) + 2\varepsilon_2 P \quad (4)$$

$$\varepsilon_b = \varepsilon_1 P + \varepsilon_2(3 - P) \quad (5)$$

$$P = 1 - \left(\frac{r_1}{r_2}\right)^3 \quad (6)$$

f is the filling factor and $\varepsilon_3$is the dielectric constant of the host medium.

In Fig. 3, the real and imaginary part of the effective dielectric constant related to the nanoparticle and sensing layer are plotted according to equations 1 and 3 for different radius of gold nanoparticles, thickness of the shell and filling factor. It can be seen that shell thickness and core radius have more effect on dielectric constant of nanoparticle (ε_e) rather than sensing layer (ε).

It can be deduced that filling factor is more dominant on the effective dielectric constant of sensing layer as shown in Fig.3.c.

To evaluate the performance and response of the proposed structure, the Transfer Matrix Method (TMM) is used [40-41]. It is a well-known approach for mathematical modeling of periodic structures and light reflection analysis in the structures similar to the proposed SPR biosensor.

In this method, for thek^{th}layer, d_k, ε_k, $and\ n_k$ are considered as the thickness, dielectric constant and refractive index respectively. The relation between the tangential fields at the first boundary and final boundary can be expressed by [42-43]

$$\begin{bmatrix} U_1 \\ V_1 \end{bmatrix} = M \begin{bmatrix} U_{N-1} \\ V_{N-1} \end{bmatrix} \quad (7)$$

Here, U_1, V_1, U_{N-1} and V_{N-1} are the tangential components of electric and magnetic fields at the boundary of the first layer and at the N^{th} layer of the structure respectively.

In TM mode, the matrix M_{ij} for the N-Layer biosensor structure can be expressed as [42-43]

$$M_{ij} = \left(\prod_{k=2}^{N-1} M_k\right)_{ij} = \begin{pmatrix} M_{11} & M_{12} \\ M_{21} & M_{22} \end{pmatrix} \quad (8)$$

In Equation 8, $M_k$is the Transfer Matrix of the k^{th}layer, which can be expressed as [42-43]

$$M_k = \begin{pmatrix} cos\beta_k & -(i\ sin\beta_k)/q_k \\ -iq_k sin\beta_k & cos\beta_k \end{pmatrix} \quad (9)$$

$$q_k = \left(\frac{\mu_k}{\varepsilon_k}\right)^{1/2} \quad (10)$$

$$\cos\theta_k = \frac{\left(\varepsilon_k - n_1^2 sin^2\theta_1\right)^{1/2}}{\varepsilon_k} \quad (11)$$

$$\beta_k = \frac{2\pi}{\lambda} n_k \cos\theta_k (z_k - z_{k-1}) = \frac{2\pi d_k}{\lambda}(\varepsilon_k - n_1^2 sin^2\theta_1)^{1/2} \quad (12)$$

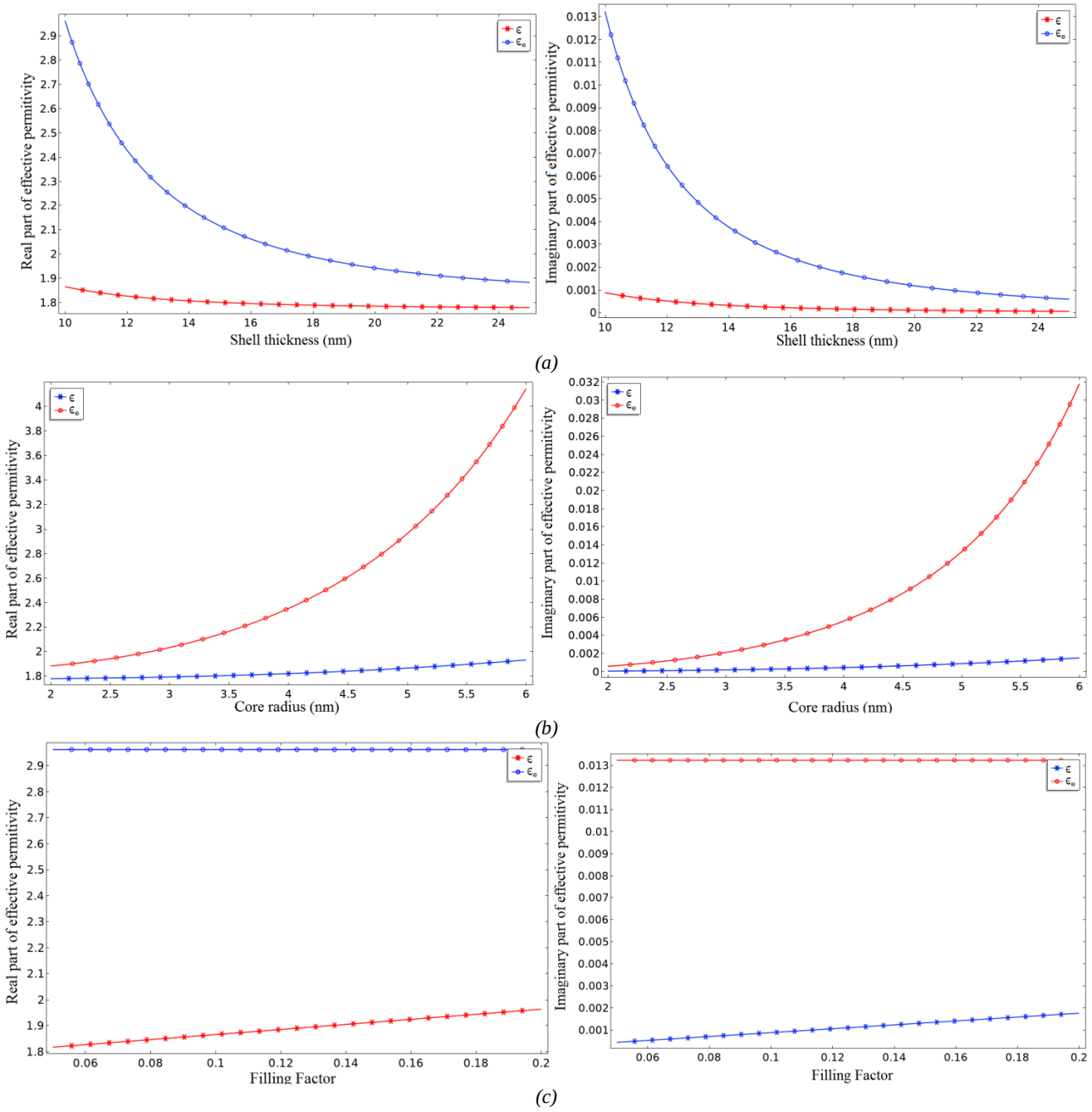

Fig. 3. The real and imaginary parts of dielectric constant of nanoparticle (ε_e) and sensing layer (ε) for different values of a) shell thickness When $f = 0.1$ and $r_1 = 5$ nm, b) core radius when $f = 0.1$ and a=10 nm and c) filling factor when a=10 nm and $r_1 = 5$ nm (color online)

Finally, the reflection coefficient and the reflection intensity in TM mode for the N-Layer biosensor is expressed as [42-43]

$$r_p = \frac{(M_{11}+M_{12}q_N)q_1-(M_{21}+M_{22}q_N)}{(M_{11}+M_{12}q_N)q_1+(M_{21}+M_{22}q_N)} \quad (13)$$

$$R_p = |r_p|^2 \quad (14)$$

Sensitivity, detection accuracy and quality factor are three main characteristics which fully describe the overall performance of biosensors. The sensitivity (S) is expressed by the ratio change of the resonance angle ($\Delta\theta_{SPR}$)to the refractive index change in the sensing medium. This parameter is defined as $S = \frac{\Delta\theta_{SPR}}{\Delta n}(^{\circ}/_{RIU})$ [44]. Detection accuracy ($D.A$) is described as the ratio change of the resonance angle ($\Delta\theta_{SPR}$)to the Full Width at Half Maximum (FWHM) according to the reflectance diagram which can be calculated as $D.A = \frac{\Delta\theta_{SPR}}{FWHM}$ [44]. The quality factor (Q.F) is expressed by the calculation of the sensitivity and FWHM as $Q.F = \frac{S}{FWHM}(RIU^{-1})$ [44].

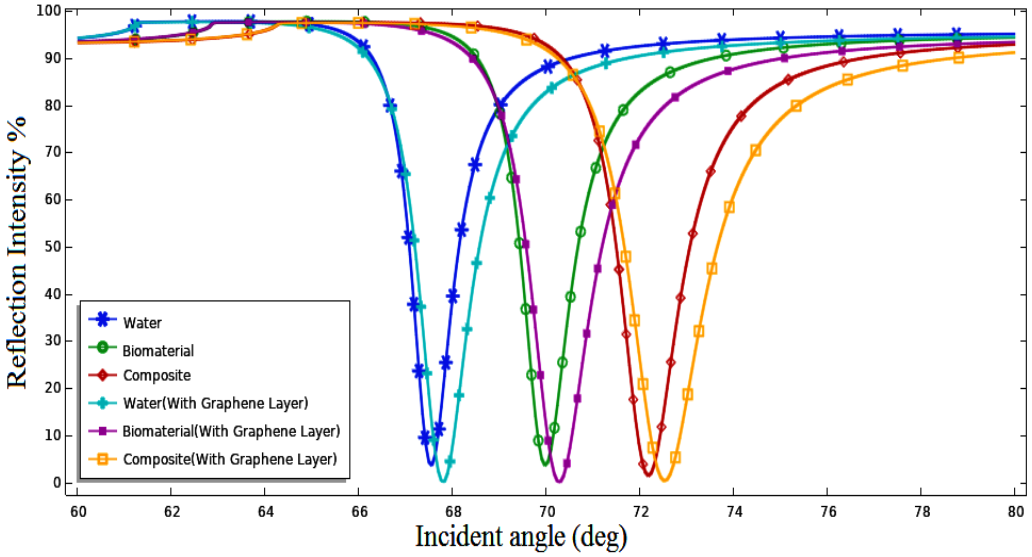

Fig. 4. Effect of graphene layer on the reflection diagram for different sensing layers; water, biomaterial and nanocomposite structure; ($r_1 = 5\ nm$, $a = 5\ nm$ and $f = 0.1$) (color online)

3. Results and discussion

In this paper, Matlab software has been used to calculate the various parameters of the proposed SPR biosensor. At the first step of simulations, as shown in Fig.4, three different cases for the sensing layer is considered; the first, completely filling the sensing layer by pure water as the reference case, the second, biomaterial being solved in water and the third, nanocomposite structure as shown in Fig. 2 for the first two ones, effective refractive index of sensing layer is considered as 1.33 and 1.35 while for the nanocomposite structure the calculation is done according to Eqs.1 and 2. To illustrate the better performance of biosensor in the case of nanocomposite structure, a layer of graphene is added and the structure is simulated again for all three cases which is depicted in Fig. 4. It is calculated that nanocomposite sensing medium results in the maximum angular shift, so better sensitivity can be obtained in the case of nanocomposite structure rather than using the biomaterial sample being solved in water.

Table 2. Refractive index change, sensitivity and angle of dip position for different cases of physical parameters of nanocomposite layer

	Core radius, $r_1(nm)$ $a = 10nm, f = 0.1$			**Shell thickness, $a(nm)$ $r_1 = 5nm, f = 0.1$.**			**Filling factor (f) $a = 10nm, r_1 = 5$.**			
Variable	2 nm	4 nm	6 nm	5 nm	11 nm	20 nm	0.05	0.1	0.15	0.2
Δn	0.0042	0.0196	0.0603	0.0042	0.0104	0.0361	0.0182	0.0361	0.0539	0.0714
Sensitivity ($^{\circ}/_{RIU}$)	107.66	125.806	149	132.01	120.932	107.69	123	129.63	141.09	155.742
Angle of Dip position (°)	68.255	70.268	76.711	72.483	69.06	68.255	70.06	72.4	75.4	78.9

As proved in previous section, the effective refractive index of nanocomposite sensing layer depends on physical parameters of the nanoparticles. Any change in the values of core radius, shell thickness and filling factor alter the effective dielectric constant of the sensing layer as shown in Fig.3.

The next simulations are carried out according to Table 2 in which different cases are considered and the corresponding refractive index change (Δn) is calculated relative to reference value of water. As mentioned before, filling factor is more dominant than the shell thickness and core radius on refractive index change.

For better evaluation of the refractive index change of Table 2 and its effect on reflection intensity diagram, Fig. 5 shows the simulation results of the biosensor structure for each case of Table 2 while setting the number of graphene layer as *L=1*. It is noted that the increment of core radius, and filling factor results in increase of incident angle dip position and its FWHM, while it is vice versa for the shell thickness as shown in Fig. 5 (b). Having calculated the sensitivity parameter and angle of dip position, two new rows are added in Table 2 for better comparison.

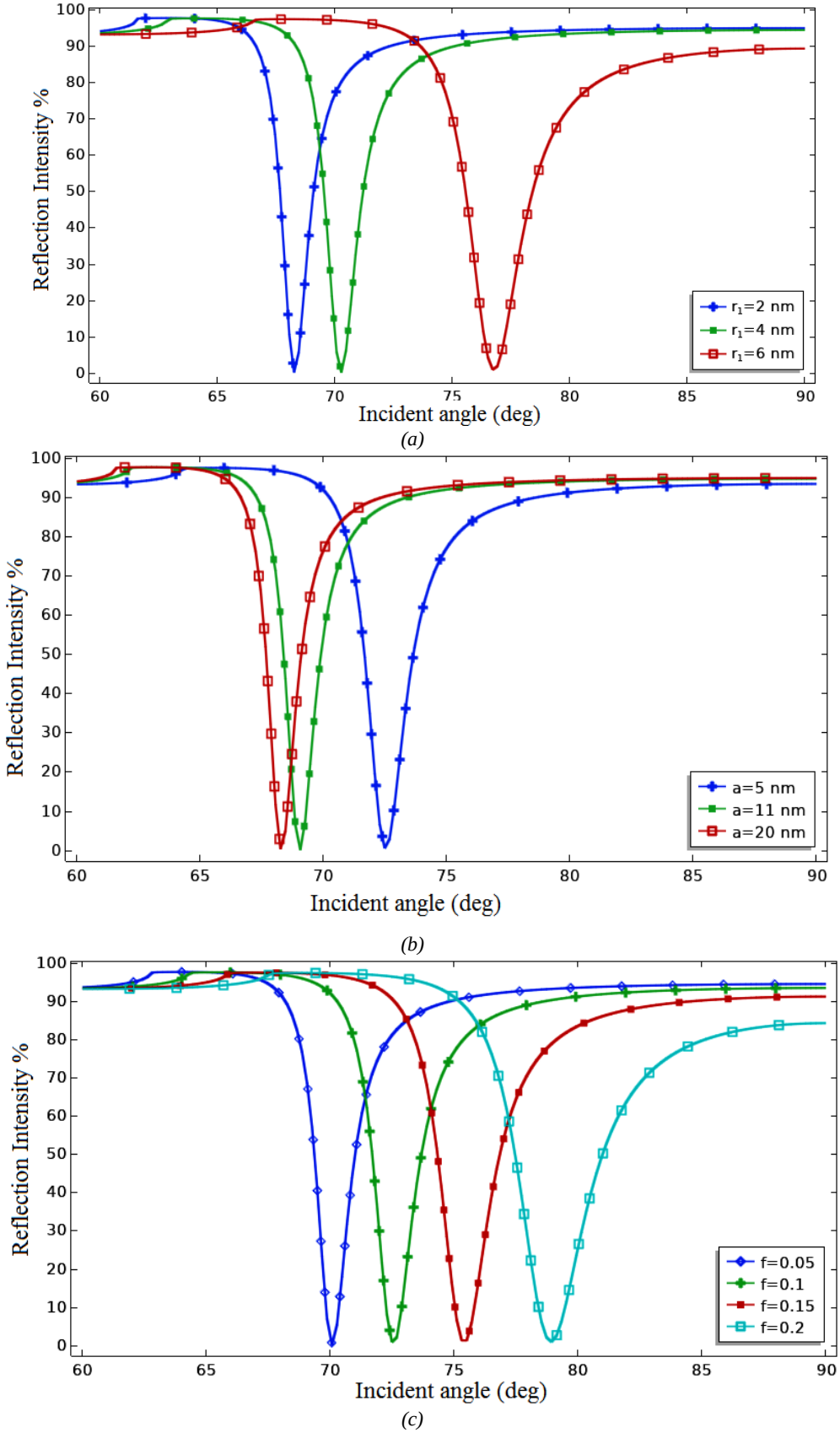

Fig. 5 The reflection intensity as a function of incident angle for the cases listed in Table 2 ($n_{host} = 1.33, L = 1$) for different values of; a)core radius, b)shell thickness and c)filling factor (color online)

Beside the physical parameter of nanoparticles and filling factor, the layer of 2D material as shown in Fig.1 and

described in Table 1, has an important effect on improving the overall performance of biosensor and should be well investigated.

As suggested in Table 1, three materials of graphene, BP and WS2 is chosen to investigate their effect on biosensor performance. Fig. 6 shows a detailed comparison of biosensor sensitivity regarding the change of both physical parameter ($\boldsymbol{r_1, a, f}$) and number of 2D material layers($\boldsymbol{L,M,N}$) for graphene, BP and WS2. The most obvious conclusion from Fig. 6 is that the higher sensitivity is associated with higher number of 2D material layers. In other words, the thicker the 2D layer, the higher the sensitivity. It is worthy to note that the limit for thickness of 2D layer is skin dept and formation of SPP wave in the structure. According to our simulations, maximum number of 3 is chosen, accordingly.

According to Fig. 6 a, b, c, and Fig. 6 g, h, i, core radius and filling factor increment result in higher values of sensitivity. Fig. 6 d, e, f shows that if the shell thickness increases the sensitivity decreases. According to Fig.6, WS2 is better suggestion for 2D material as it shows higher sensitivity than graphene and BP. Moreover, single layer of graphene shows the lower sensitivity than the other cases in Fig. 6. The range of sensitivity change in Fig. 6 is between $107.666(^{\circ}/_{RIU})$ and $286.9(^{\circ}/_{RIU})$ for the single layer of graphene ($r_1 = 2\ nm, a = 5\ nm, f = 0.1$) and three layers of WS2 ($r_1 = 6\ nm, a = 5\ nm, f = 0.1$), respectively.

Along with sensitivity parameter, similar figures for D.A and Q.F can be depicted. Instead of showing more figures, a summary and important results are shown in Table 3. The physical parameters of nanoparticles are set to a=5 nm, r_1=5 nm,$n_{host} = 1.33$, f=0.1 and for different type of 2D materials and different number of their layers, the biosensor performance parameters of S, D.A and Q.F are calculated in Table 3. According to Table 3, the highest sensitivity and lowest values of D.A and Q.F SPR biosensor are related to WS2 with three layers. Also, the lowest sensitivity and the highest values of D.A and Q.F are related to a single-layer grapheme.

As a result, be selecting the appropriate structural parameters for the sensing layer and selecting the type and thickness of 2D-material layers, a SPR biosensor with the desired properties can be designed to detect biomolecules and biomaterial samples.

Finally, a comparison is made between the performance of the proposed structure and other references listed in Table 4 which shows higher sensitivity and better quality factor of our proposed structure.

Table 3. Calculated sensor parameters for $a = 5nm, r_1 = 5nm, f = 0.1$.

Type of 2D Materials	No. of layers	$S(^{\circ}/_{\boldsymbol{RIU}})$	D.A	Q.F($\boldsymbol{RIU^{-1}}$)
Graphene	1	130.016	2.3565	65.2797
	2	133.59	2.0508	56.8096
	3	136.49	1.8360	50.8611
Black phosphorous(BP)	1	132.53	2.7809	77.1131
	2	139.57	2.5980	71.9682
	3	145.23	2.4232	67.1242
Tungsten disulfide(WS2)	1	139.89	1.9427	53.8168
	2	158.76	1.5881	43.9937
	3	260.38	1.0375	28.7407

Table 4. Comparison of our biosensor with others reported ones in the literatures

References	**Biosensor configuration**	**Enhancement strategy**	**Wavelength (nm)**	**$S(^{\circ}/_{\boldsymbol{RIU}})$**	**Q.F($\boldsymbol{RIU^{-1}}$)**
[45]	Kretschmann	Using Graphene and WS2	633	95.71	25.19
[46]	Kretschmann	Using Ag–MoS2–grapheme	680	190	18.68
[33]	otto	Using MoS2/Graphene-nanocomposite	633	200	11.51
Proposed work	Kretschmann	Using Core-shell nanostructure and 2D material layer	633	260.385	28.74

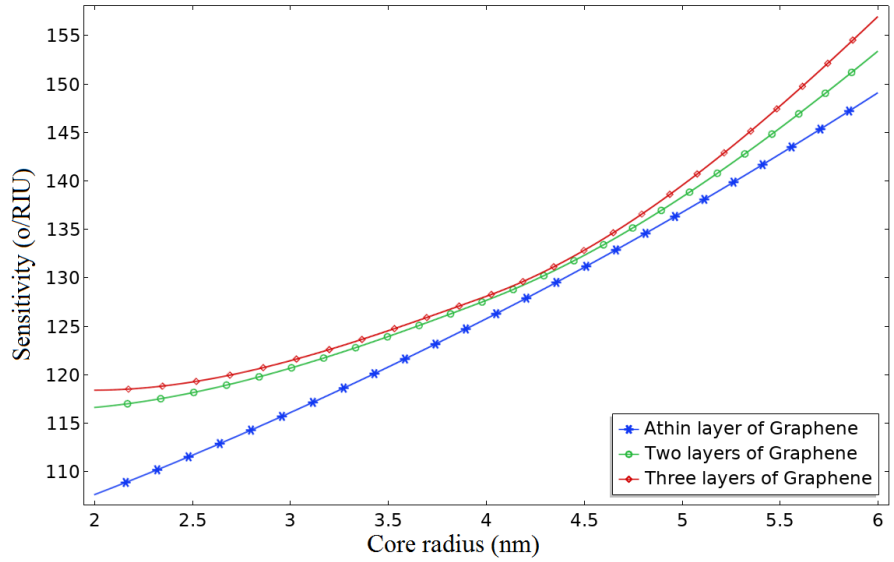
Sensitivity (o/RIU)
Core radius (nm)
Athin layer of Graphene
Two layers of Graphene
Three layers of Graphene

(a)

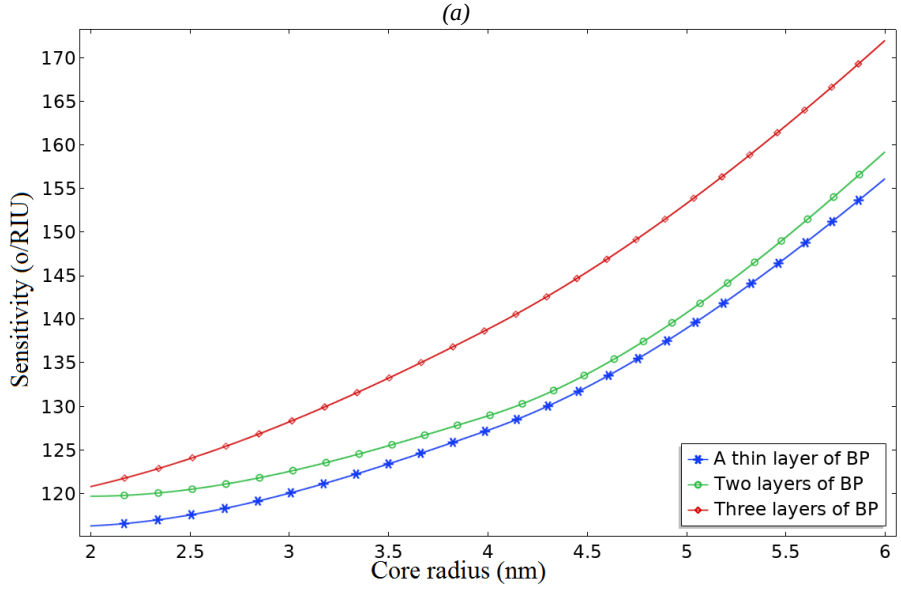
Sensitivity (o/RIU)
Core radius (nm)
A thin layer of BP
Two layers of BP
Three layers of BP

(b)

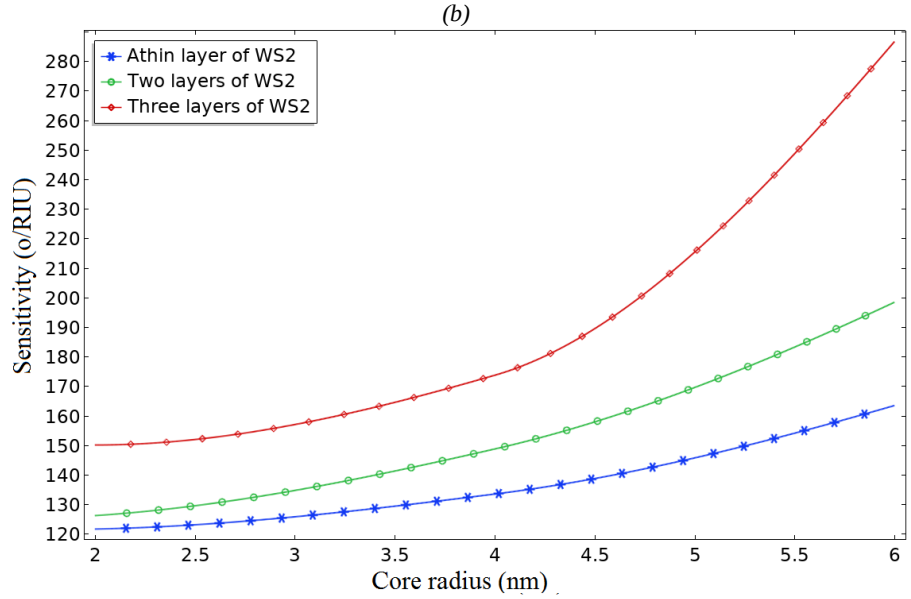
Sensitivity (o/RIU)
Core radius (nm)
Athin layer of WS2
Two layers of WS2
Three layers of WS2

(c)

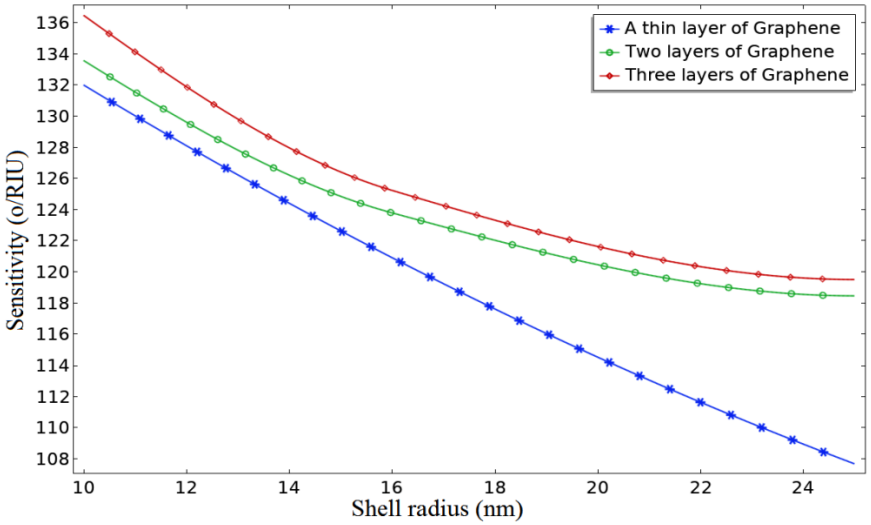
A thin layer of Graphene
Two layers of Graphene
Three layers of Graphene
Sensitivity (o/RIU)
Shell radius (nm)

(d)

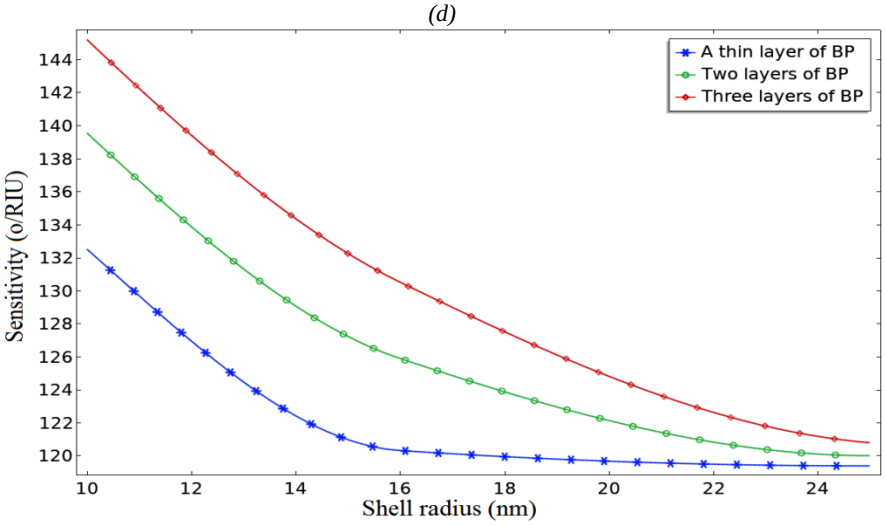
A thin layer of BP
Two layers of BP
Three layers of BP
Sensitivity (o/RIU)
Shell radius (nm)

(e)

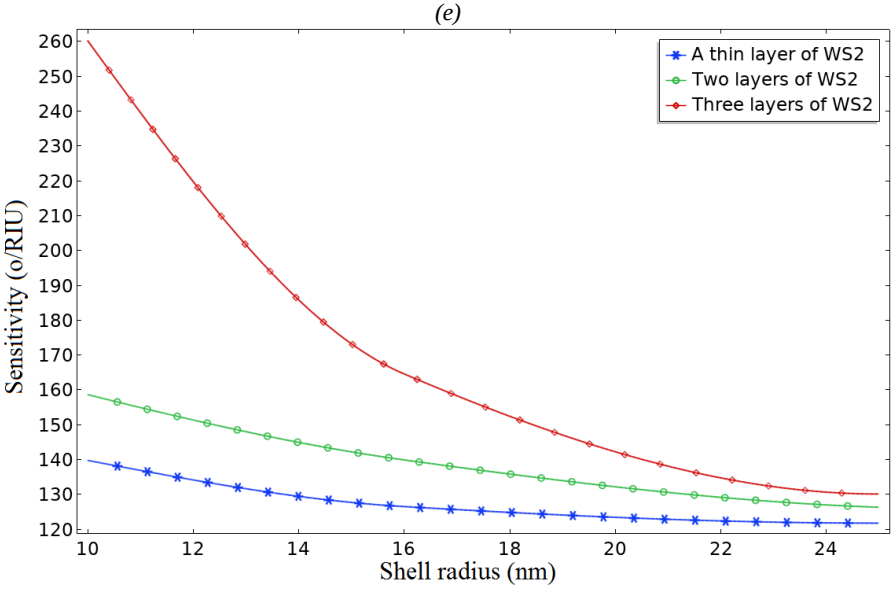
A thin layer of WS2
Two layers of WS2
Three layers of WS2
Sensitivity (o/RIU)
Shell radius (nm)

(f)

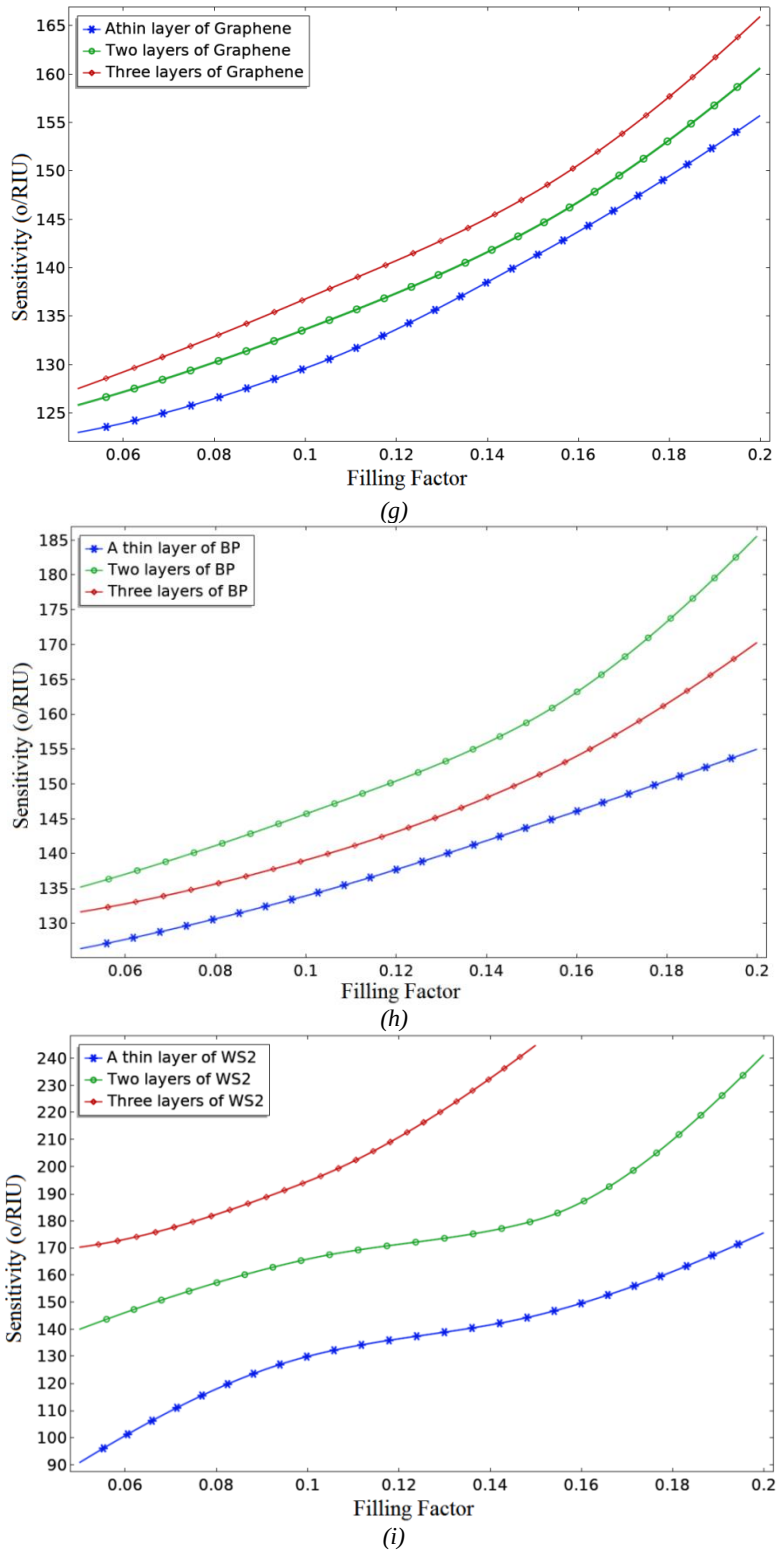

Fig. 6 Effect of number of different 2D layers (graphene, BP and WS2) on the sensitivity of the proposed structure as the function of; (a,b,c) core radius, (d,e,f) shell thickness and (g,h,i) filling factor (color online)

4. Conclusion

A five-layer Surface Plasmon Resonance (SPR) biosensor based on Kretschmann configuration for biomaterial sample detection is proposed. By employing nanoparticles with core-shell structure as an active material in the sensing layer and using a 2D material layer, the performance and sensitivity of the proposed biosensor are improved. The Maxwell-Garnet theory is also used to investigate and calculate the effective parameters of the sensing layer. The simulation results show that by changing the nanaoparticle core radius, the shell thickness of the

biomaterial sample and filling factor, as effective physical parameters in the sensing. In addition, the reported SPR biosensor has a simple structure, high sensitivity and proper performance, so that this structure can be used in various fields of medicine, biology and healthcare.

References

[1] S. Ghorbani , M. Sadeghi, Z. Adelpour, Laser Phys. **30**, 026204 (2020) .
[2] F. S. Ligler, C. R. Taitt, L. C. Shriver-Lake, K. E. Sapsford, Y. Shubin, J. P. Golden, Anal. Bioanal. Chem. **377**, 469(2003).
[3] M. Saleh, M. F. O. Hameed, N. F. F. Areed, S. S. A. Obayya, Appl. Comput. Electromagn. Soc. J. **31,** 836 (2016).
[4] N. F. F. Areed, M. F. O. Hameed, S. S. A. Obayya, Opt. Quantum Electron. **49**, 1 (2017).
[5] A. Lahav, M. Auslender, I. Abdulhalim, Opt. Lett. **33**, 2539 (2008).
[6] L. Wu, H. S. Chu, W. S. Koh, E. P. Li, Opt. Express **18**, 14395 (2010).
[7] S. Zeng, S. Hu, J. Xia, T. Anderson, X. Q. Dinh, X. M. Meng, P. Coquet, K. T. Yong, Sens. Actuators B **207**, 801 (2015).
[8] H. Ditlbacher, J. R. Krenn, F. R. Aussenegg, Appl. Phys. Lett. **81**, 1762 (2002).
[9] P. Pattnaik, Appl. Biochem. Biotechnol. **126**, 79 (2005).
[10] Widayanti, K. Abraha, A. B. S. Utomo, Biosensors **8**, 75 (2018).
[11] Z. Salamon, H. A. Macleod, G. Tollin, Biochim. Biophys. Acta **1331**, 131 (1997).
[12] L. Wu, H. S. Chu, W. S. Koh, E. P. Li, Opt. Express **18**, 14395 (2010).
[13] M. Frasconi, C. Tortolini, F. Botrè, F. Mazzei, Anal. Chem. **82**, 7335 (2010).
[14] R. P. Liang, G. H. Yao, L. X. Fan, J. D. Qiu, Anal. Chim. Acta **737**, 22 (2012).
[15] W. C. Law, K. T. Yong, A. Baev, P. N. Prasad, ACS Nano. **5**, 4858 (2011).
[16] K. M. Byun, D. Kim, S. J. Kim, Proc. SPIE. **5703**, 61 (2005).
[17] A. Otto, Z. Phys. A Hadrons Nuclei. **216**, 398 (1968).
[18] J. R. Sambles, G. W. Bradbery, F. Yang, Contemp. Phys. **32**, 173 (1991).
[19] O. Stephan, D. Taverna, M. Kociak, L. Henrard, K. Suenaga , C. Colliex, AIP Conference Proceedings. **633**, 326 (2002).
[20] P. Englebienne, A. V. Hoonacker, M. Verhas, J. Spectrosc. **17**, 255 (2003).
[21] H. O. Churchill, P. Jarilloherrero, Nat. Nanotechnol. **9**, 330 (2014).
[22] A. S. Rodin, A. Carvalho, A. H. Castro Neto, Phys. Rev. Lett. **112**, 176801 (2014).
[23] C. Cong, J. Shang, X. Wu, B. Cao, N. Peimyoo, C. Qiu, L. Sun, T. Yu, Adv. Opt. Mater. **2**, 131 (2014).
[24] S. Singh, A. K. Sharma, P. Lohia, D. K. Dwivedi, Optik **244**, 167618 (2021).
[25] Y. Singh, M. K. Paswan, S. K. Raghuwanshi, Plasmonics **16**, 1781 (2021).
[26] M. Setareh, H. Kaatuzian, Superlattices Microstruct. **153**, 106867 (2021).
[27] M. M. Rahman, M. M. Rana, M. S. Rahman, M. S. Anower, M. A. Mollah, A. K. Paul, Optical Materials **107**, 110123 (2020).
[28] Z. Lin, S. Chen, C. Lin, Sensors **20**, 2445 (2020).
[29] L. Wu, Y. Jia, L. Jiang, J. Guo, X. Dai, Y. Xiang, D. Fan, J. Lightwave Technol. **35**, 82 (2017).
[30] M. A. Ordal, R. J. Bell, R. W. Alexander, L. L. Long, M. R. Querry, Appl. Optic. **24**,4493 (1985).
[31] M. S. Rahman, M. S. Anower, M. K. Rahman, M. R. Hasan, M. B. Hossain, M. I. Haque, Optik **140**, 989 (2017).
[32] Q. Ouyang, S. Zeng, L. Jiang, L. Hong, G. Xu, X. Q. Dinh, J. Qian, S. He, J. Qu, P. Coquet, K. T. Yong, Sci. Rep. **6**,28190 (2016).
[33] H. Vahed, C. Nadr, Optical Materials **88**, 161 (2019)
[34] S. Ghorbani, M. Sadeghi, Z. Adelpour, Laser Phys. **30**, 086201 (2020).
[35] U. K. Chettiar, N. Engheta, Opt. Express **20**, 22976 (2012).
[36] Antonio J. S. Barroso, Luis A. Gómez-Malagón, Plasmonics **9**, 193 (2014).
[37] R. J. Gehr, R. W. Boyd, Chem. Mater. **8**,1807 (1996)
[38] Q. Xue, J. Mater. Sci. Technol. **16,** 367 (2000).
[39] A. E. Neeves, M. H. Birnboim, J. Opt. Soc. Am. B **6**, 787 (1989).
[40] J. B. Maurya, Y. K. Prajapati, V. Singh, J. P. Saini, R. Tripathi R, Opt. Commun. **359**, 426 (2016).
[41] J. B. Maurya, Y. K. Prajapati, V. Singh, J. P. Saini, R. Tripathi, Opt. Quantum Electron. **47**, 3599 (2015).
[42] J. Zhao, X. Y. Zhang, C. R. Yonzon, A. J. Haes, R. P. Van Duyne, Nanomedicine **1**, 219 (2006).
[43] M. Saifur Rahman, Md. Rabiul Hasan, Khaleda Akter Rikta, M. S. Anower, Optical Materials **75**, 567 (2018).
[44] M. Saifur Rahman, Md. Shamim Anower, Md. Rabiul Hasan, Md. Biplob Hossain, Md. Ismail Haque Md, Opt. Commun. **396**, 36 (2017).
[45] M. Saifur Rahman, Md. Rabiul Hasan, Khaleda Akter Rikta, M. S. Anower, Optical Materials **75**, 567 (2018).
[46] H. Vahed, C. Nadri, Opt. Quantum Electron. **51**, 1 (2019).

*Corresponding author: S.ghorbani2010@gmail.com